Supporting Information

for

Remarkable brain penetration of cyclopentadienyl $M(CO)_3^+$ (M = ^{99m}Tc, Re) derivatives of benzothiazole and benzimidazole paves the way for their application as diagnostic, with Single Photon Emission Computed Tomography (SPECT), and therapeutic agents for Alzheimer's disease

Marina Sagnou,[§] Barbara Mavroidi,[§] Antonio Shegani,[‡] Maria Paravatou-Petsotas,[‡] Catherine Raptopoulou[#], Vassilis Psycharis,[#] Ioannis Pirmettis,[‡] Minas S. Papadopoulos,[‡] Maria Pelecanou*[§]

Contents	page
Figure S1. IR spectra of **Fe-3** and **Re-3**	S2
Figure S2. ^{1}H and ^{13}C NMR spectra of **Fe-1**	S3
Figure S3. ^{1}H and ^{13}C NMR spectra of **Re-1**	S4
Table S1. ^{1}H and ^{13}C chemical shifts for **Fe1 - Fe-3**.	S5
Table S2. ^{1}H and ^{13}C chemical shifts for **Re-1 - Re-3**	S6
Figure S4. Absorbance and fluorescence spectra for **Re-1 - Re-3**	S7
Table S3. Geometric parameters (Å, °) for **Fe-1**	S8
Table S4. Geometric parameters (Å, °) for **Re-1**	S9
Intermolecular interactions in the structure of **Fe-1**	S10
Figure S5. Layers of clusters in **Fe-1**	S10
Intermolecular interactions in the structure of **Re-1**	S11
Figure S6. Dimers of clusters in the structure of **Re-1**	S11
Figure S7. Layers of clusters in the structure of **Re-1**	S12
Figure S8. 3D Arrangement of clusters in the structure of **Re-1**	S13
Figure S9. HPLC chromatograms of Re and ^{99m}Tc complexes	S14
Table S5. Stability studies of ^{99m}Tc and Re complexes	S15
Figure S10. Stability of **^{99m}Tc-1 - ^{99m}Tc-3** in rat plasma	S16
Figure S11. Amyloid plaque staining with **Re-1**	S17
Table S6. Biodistribution of **^{99m}Tc-1** in Tg and wt mice	S18
Figure S12. Amyloid plaque staining in Tg brain slices with thioflavin S	S19
Figure S13. MTT studies with **Re-1 - Re-3**	S20
Figure S14. CD spectra of **Re-1 - Re-3**	S21
Figure S15. CD spectra of the aggregation of Aβ42	S22

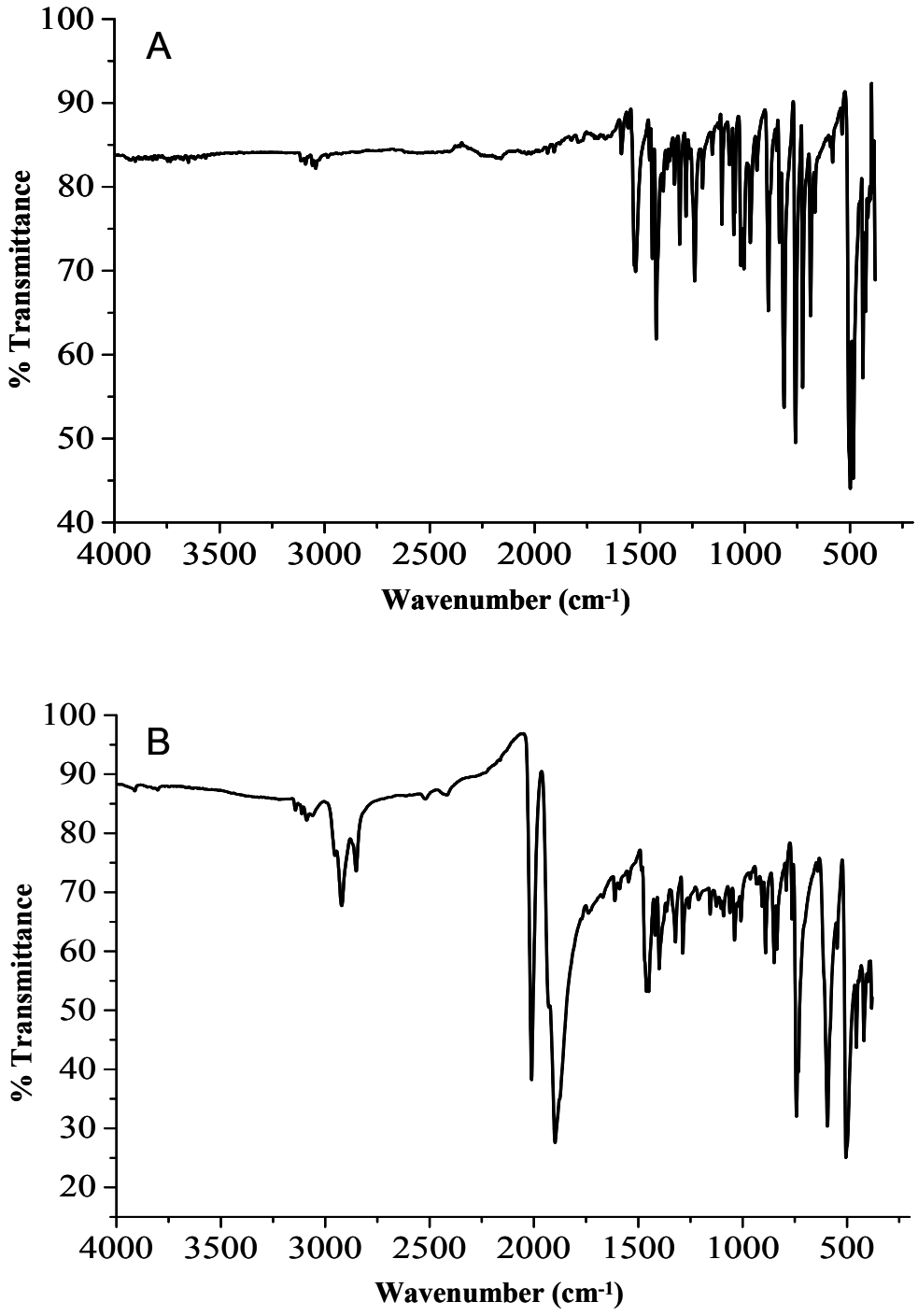

Figure S1. IR spectra (4000 - 380 cm^{-1}) of (A) **Fe-3** and (B) **Re-3** complexes.

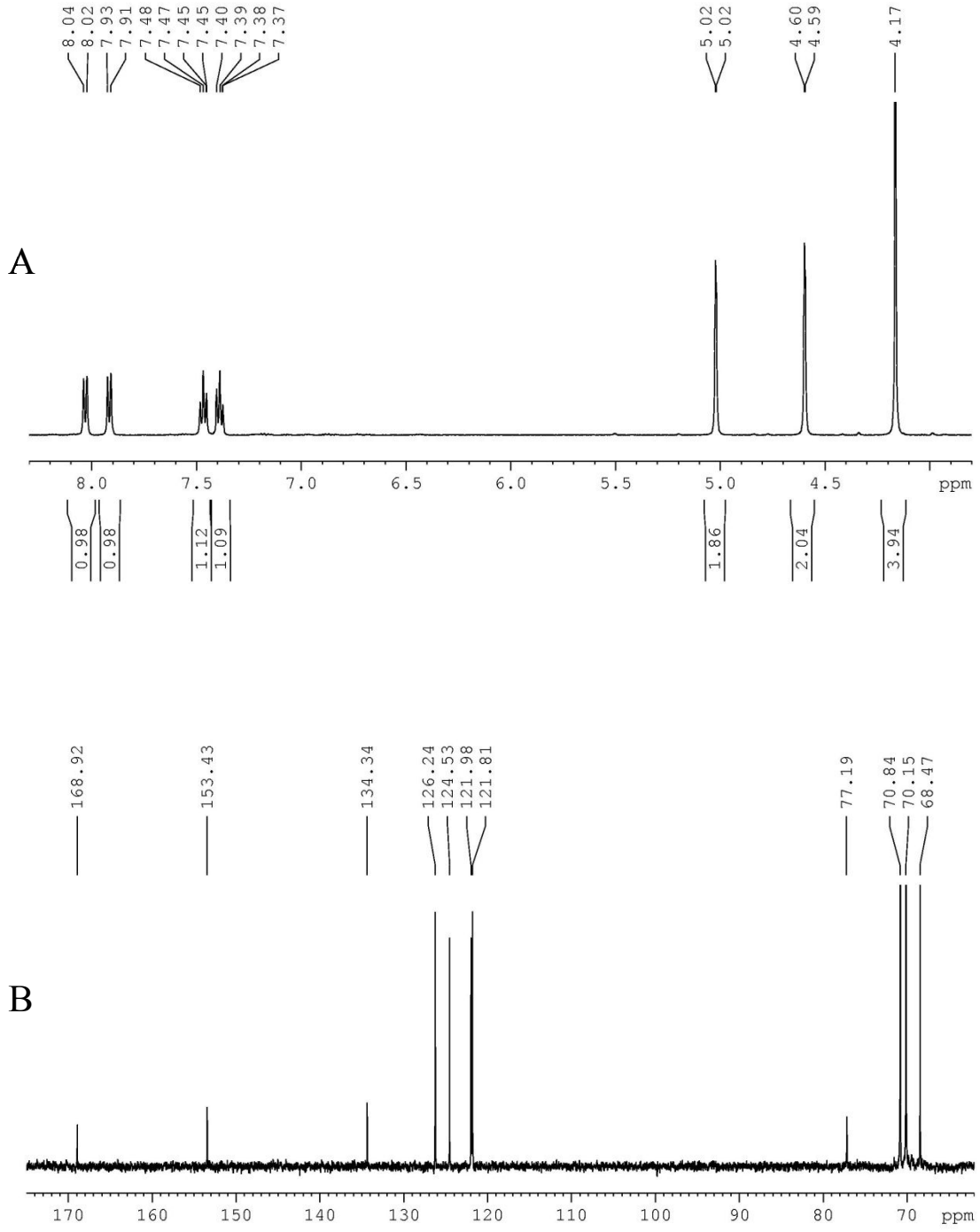

Figure S2. (A) ^{1}H (range 8.30 - 3.80 ppm) and (B) ^{13}C (range 175.0 - 62.0 ppm) NMR spectra for **Fe-1** in DMSO-d_6 at 25 °C.

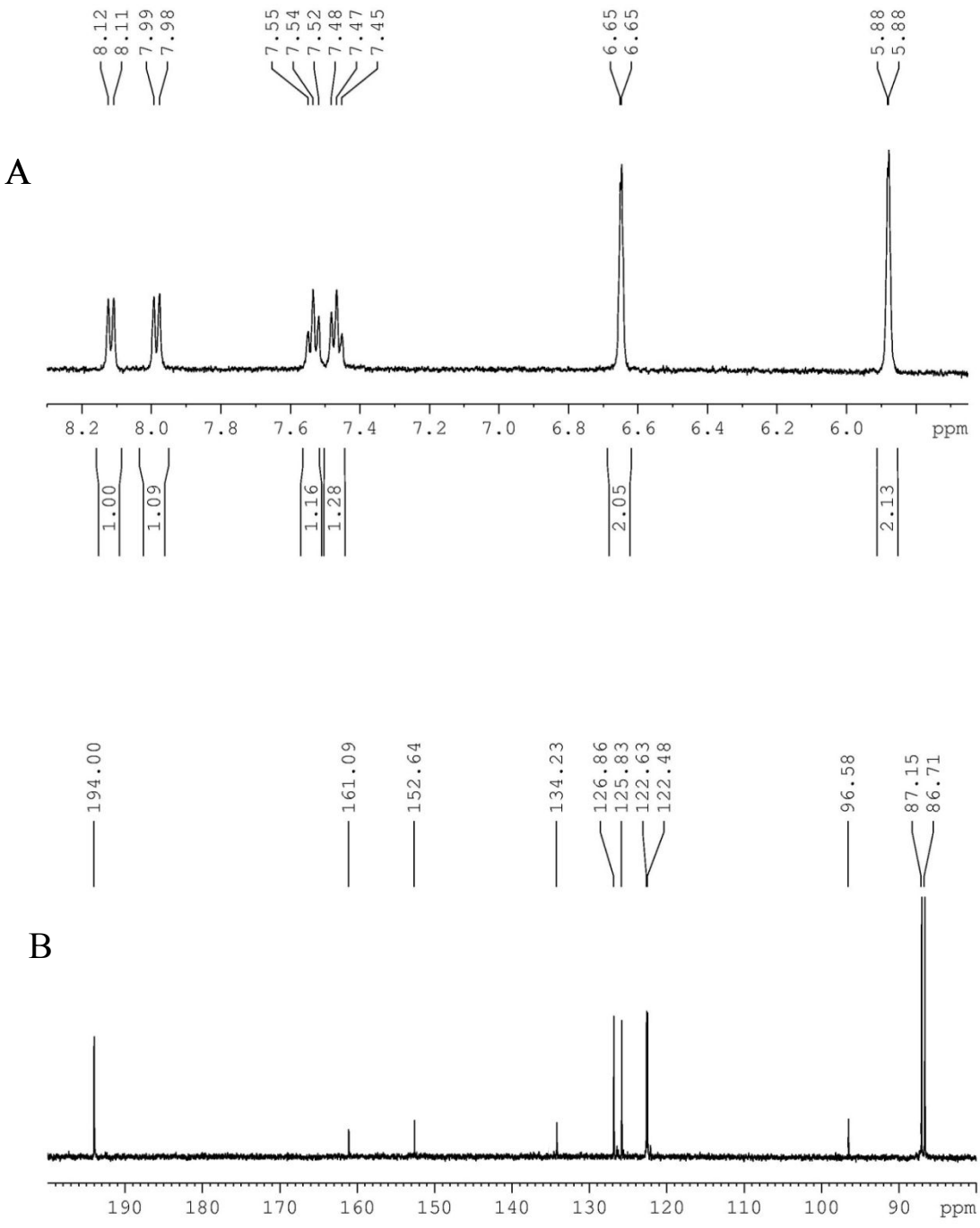

Figure S3. (A) ^{1}H (range 8.30 - 5.65 ppm) and (B) ^{13}C (range 200.0 - 80.0 ppm) NMR spectra for **Re-1** in DMSO-d_6 at 25 °C.

Table S1. ^{1}H and ^{13}C NMR chemical shifts for the ferrocenyl derivatives **Fe-1**, **Fe-2** and **Fe-3** in DMSO-d_6 at 25 °C. The atom numbering is shown in the structure below

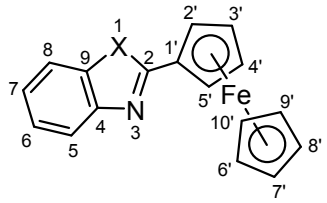

Fe-1 X = S
Fe-2 X = NH
Fe-3 X = NCH_3

^{1}H	**Fe-1**	**Fe-2**	**Fe-3**	**^{13}C**	**Fe-1**	**Fe-2**	**Fe-3**
H-5	8.03	7.54	7.56	C-2	168.92	152.90	152.74
H-6	7.38	7.11	7.17	C-4	153.43	143.98	142.58
H-7	7.47	7.14	7.22	C-5	121.98	117.90	118.04
H-8	7.92	7.44	7.54	C-6	124.53	121.02	121.50
H-10	--	--	4.03	C-7	126.24	121.46	121.52
H-2'/H-5'	5.02	5.03	4.99	C-8	121.81	110.53	109.72
H-3'/H-4'	4.60	4.47	4.53	C-9	134.34	134.71	136.71
H-6'-H-10'	4.17	4.10	4.21	C-10	--	--	31.20
NH	--	12.35	--	C-1'	77.19	74.30	74.05
				C-2'/C-5'	68.47	67.26	68.78
				C-3'/C-4'	70.84	69.66	69.80
				C6'- C-10'	70.15	69.32	69.25

Table S2. ^{1}H and ^{13}C NMR chemical shifts for the **Re-1**, **Re-2** and **Re-3** complexes in DMSO-d_6 at 25 °C. The atom numbering is shown in the structure below

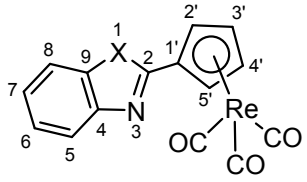

Re-1 X = S
Re-2 X = NH
Re-3 X = NCH_3

^{1}H	**Re-1**	**Re-2**	**Re-3**	**^{13}C**	**Re-1**	**Re-2**	**Re-3**
H-5	7.98	7.59	7.62	C-2	161.09	145.49	145.88
H-6	7.53	7.19	7.23	C-4	152.64	143.14	141.80
H-7	7.47	7.21	7.28	C-5	122.63	118.70	118.83
H-8	8.11	7.50	7.60	C-6	126.86	121.83	122.19
H-10	--	--	3.88	C-7	125.83	122.83	122.72
H-2'/H-5'	6.65	6.50	6.53	C-8	122.48	111.22	110.34
H-3'/H-4'	5.88	5.85	5.90	C-9	134.23	134.22	136.48
NH	--	12.78	--	C-10	--	--	31.45
				C-1'	96.58	94.95	94.00
				C-2'/C-5'	87.15	85.14	87.36
				C-3'/C-4'	86.71	86.19	86.29
				C≡O	194.00	194.30	194.17

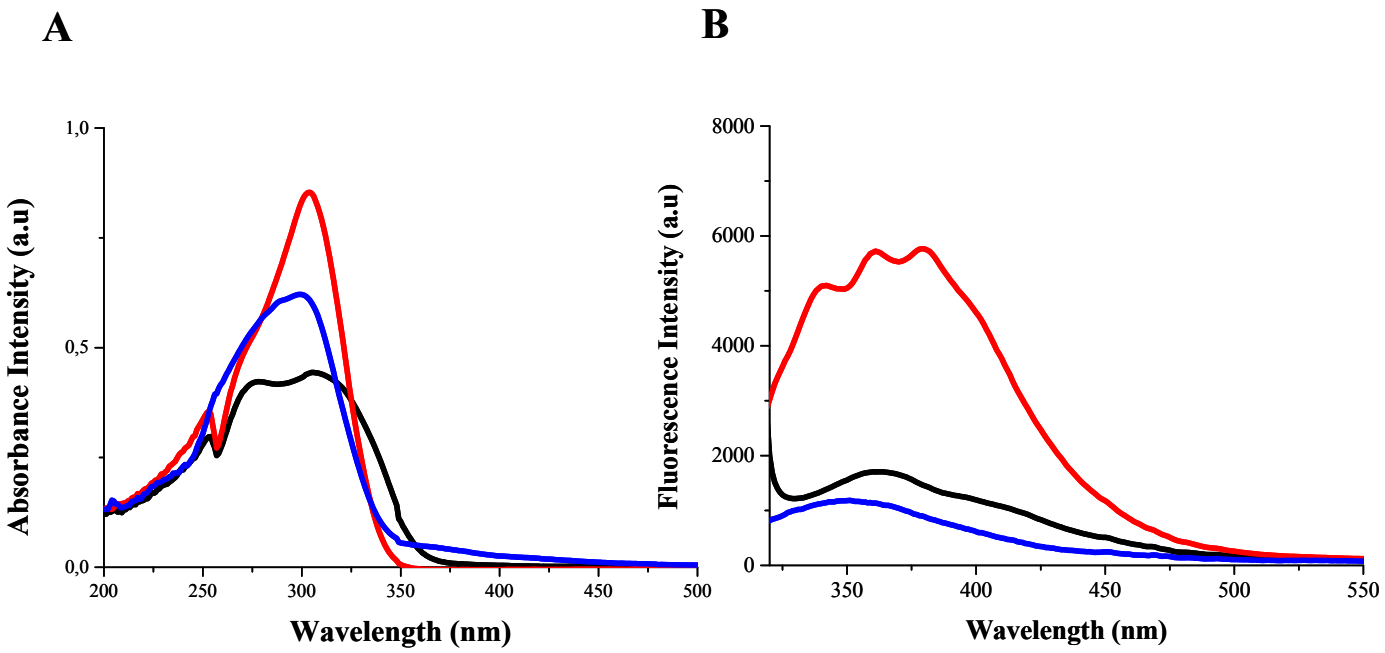

Figure S4. (A) Absorbance (200 – 500 nm) and (B) fluorescence spectra (320 - 550 nm, after excitation at 310 nm) of **Re-1** (black line), **Re-2** (red line) and **Re-3** (blue line) complexes (50 μM) in DMSO.

Table S3. Geometric parameters (Å, º) for compound **Fe-1**

Fe1—C1	2.0512 (16)	Fe1—C6	2.0351 (16)
Fe1—C2	2.0466 (16)	Fe1—C7	2.0395 (16)
Fe1—C3	2.0441 (17)	Fe1—C8	2.0455 (17)
Fe1—C4	2.0449 (16)	Fe1—C9	2.0425 (16)
Fe1—C5	2.0520 (16)	Fe1—C10	2.0424 (15)
C1—C2	1.417 (2)	C6—C7	1.420 (3)
C2—C3	1.412 (3)	C7—C8	1.423 (3)
C3—C4	1.417 (3)	C8—C9	1.426 (2)
C4—C5	1.417 (2)	C9—C10	1.439 (2)
C1—C5	1.417 (2)	C6—C10	1.438 (2)
C10—C11	1.458 (2)	C12—C13	1.399 (2)
N1—C11	1.300 (2)	C13—C14	1.381 (3)
N1—C12	1.397 (2)	C14—C15	1.397 (3)
S1—C17	1.7418 (16)	C15—C16	1.387 (3)
S1—C11	1.7576 (15)	C16—C17	1.395 (2)
C12—C17	1.407 (2)		
C5—C1—C2	107.93 (15)	C7—C6—C10	107.60 (15)
C3—C2—C1	108.04 (15)	C6—C7—C8	108.93 (15)
C2—C3—C4	108.18 (15)	C7—C8—C9	107.94 (16)
C3—C4—C5	107.84 (16)	C8—C9—C10	107.86 (15)
C1—C5—C4	108.01 (15)	C6—C10—C9	107.66 (15)

Table S4. Geometric parameters (Å, º) for compound **Re-1**

Re1—C1	1.921 (13)	C6—C7	1.413 (17)
Re1—C2	1.889 (11)	C7—C8	1.431 (14)
Re1—C3	1.909 (12)	C4—C8	1.420 (13)
C1—O1	1.143 (14)	C8—C9	1.457 (13)
C2—O2	1.148 (14)	N1—C9	1.490 (12)
C3—O3	1.139 (13)	N1—C10	1.450 (11)
Re1—C4	2.314 (9)	S1—C9	1.712 (9)
Re1—C5	2.293 (11)	S1—C11	1.677 (11)
Re1—C6	2.297 (11)	C10—C11	1.420 (13)
Re1—C7	2.288 (9)	C11—C12	1.395 (15)
Re1—C8	2.318 (8)	C12—C13	1.50 (3)
C4—C5	1.418 (16)	C13—C14	1.37 (2)
C5—C6	1.39 (2)	C14—C15	1.25 (2)
		C10—C15	1.410 (15)
C2—Re1—C1	89.5 (5)	C6—C5—C4	108.0 (11)
C3—Re1—C1	88.7 (5)	C5—C6—C7	109.4 (11)
C2—Re1—C3	89.2 (5)	C6—C7—C8	107.1 (11)
C5—C4—C8	108.1 (11)	C4—C8—C7	107.2 (9)

Intermolecular interactions in the structure of compound Fe-1

In the structure of **Fe-1** the clusters form chains along the a crystallographic axis (Figure-S5) through π ···π interactions of the five member ring (defined by C6,…, C10 atoms) with the phenyl ring (defined by C12,….C17 atoms) of the ligand with the distance of the centroid of the first ring from the second to be 3.453 (5) Å and the angle between them is 10.18(6)º. These chains farther interact through C16-H16···N1′ hydrogen bonds [C16-H16: 0.95(2) Å, H16···N1′: 2.61(2)Å, C16···N1′: 3.364(2)Å, C16-H16-N1′: 137(2)º, symmetry code (′): x, 0.5-y, 0.5+z] thus forming layers parallel to the (010) planes (Figure-S5). These layers are stacked along c-axis interacting through weak van Der Waal Contacts.

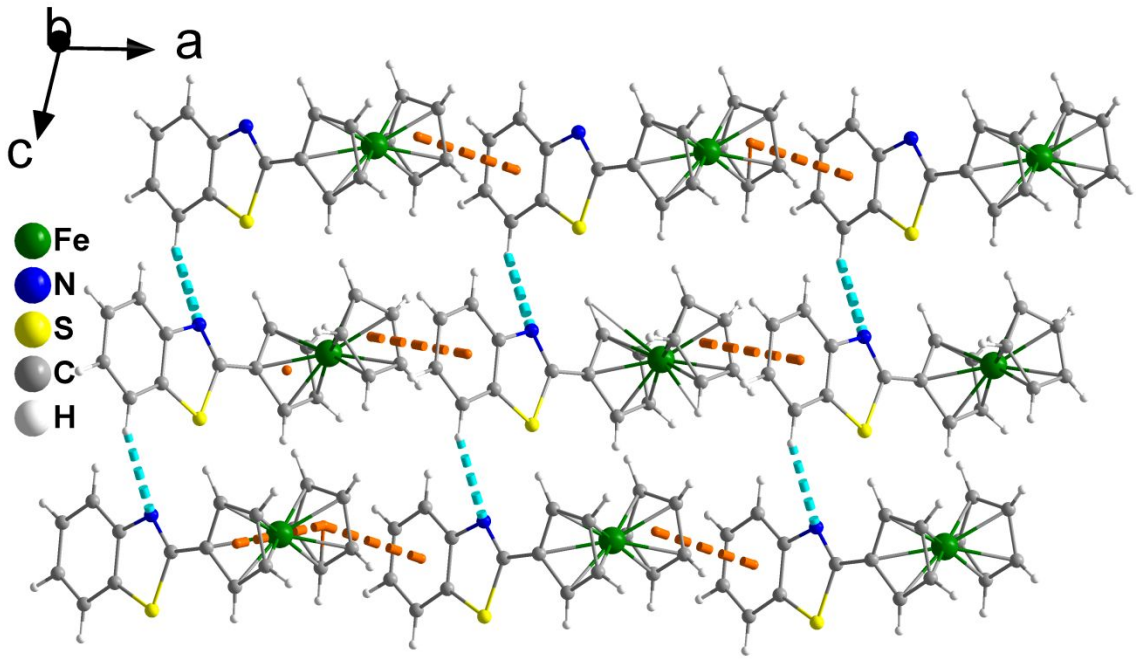

Figure S5. Layers of clusters in **Fe-1** parallel to the (010) plane. Dashed cyan and orange lines represent C16-H16···N1 and π ···π intermolecular interactions respectively.

Intermolecular interactions in the structure of compound Re-1

In the structure of **Re-1** centrosymmetrically related clusters form dimers, (Figure S6) through π ···π intermolecular interactions of the phenyl rings of the ligands (the intradimer distance of ligand phenyl ring planes related by the symmetry operation 1-x, -y, -z, is 3.53(2) Å). The ligands of neighboring dimers interact further through π ···π interactions (the interdimer distance of planes related by the symmetry operation -x,1-y, -z, is 3.560(7)) and are stacked along the [-110] crystallographic direction forming chains (Figure 3), which through S1···S1′′ contacts [3.540(3)Å, symmetry code (′′): 1-x, 1-y, -z] and C4-H4···S1′′′ intermolecular interactions [C4-H4: 0.93(1)Å, H4···S1′′′: 2.993(3)Å, C4···S1′′′: 3.64(1)Å, C4-H4-S1′′′: 128(1)°, symmetry code (′′′): -1+x, y, z] extent to layers parallel to the (001) plane (Figure S7). These layers interact through C5-H5···O2* hydrogen bonds along the [011] crystallographic direction [C5-H5:0.93(1)Å , H5···O2*:2.502(9)Å , C5···O2*: 3.32(1)Å, C5-H5-O2*: 147(1)°, symmetry code (*): -1-x, 1-y, 1-z] and thus the 3D architecture of the structure is build (Figure S8).

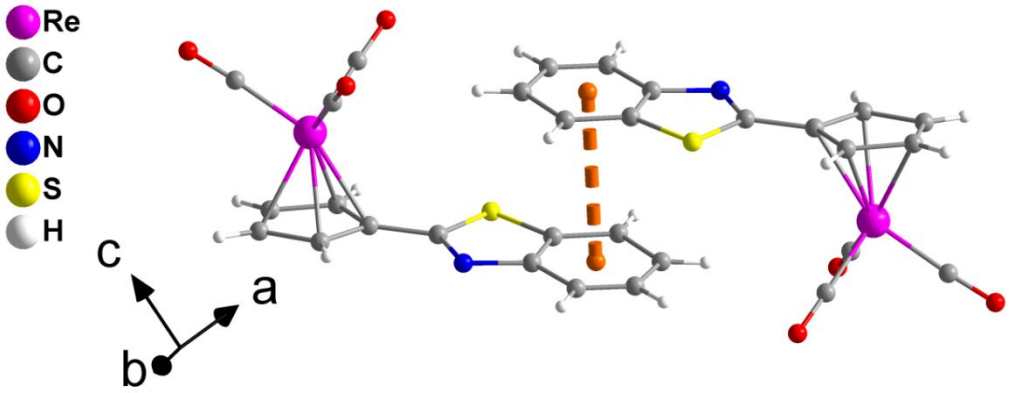

Figure S6. Dimers of clusters in the structure of **Re-1**. Dashed orange lines represent π ···π intradimer interactions of the phenyl rings.

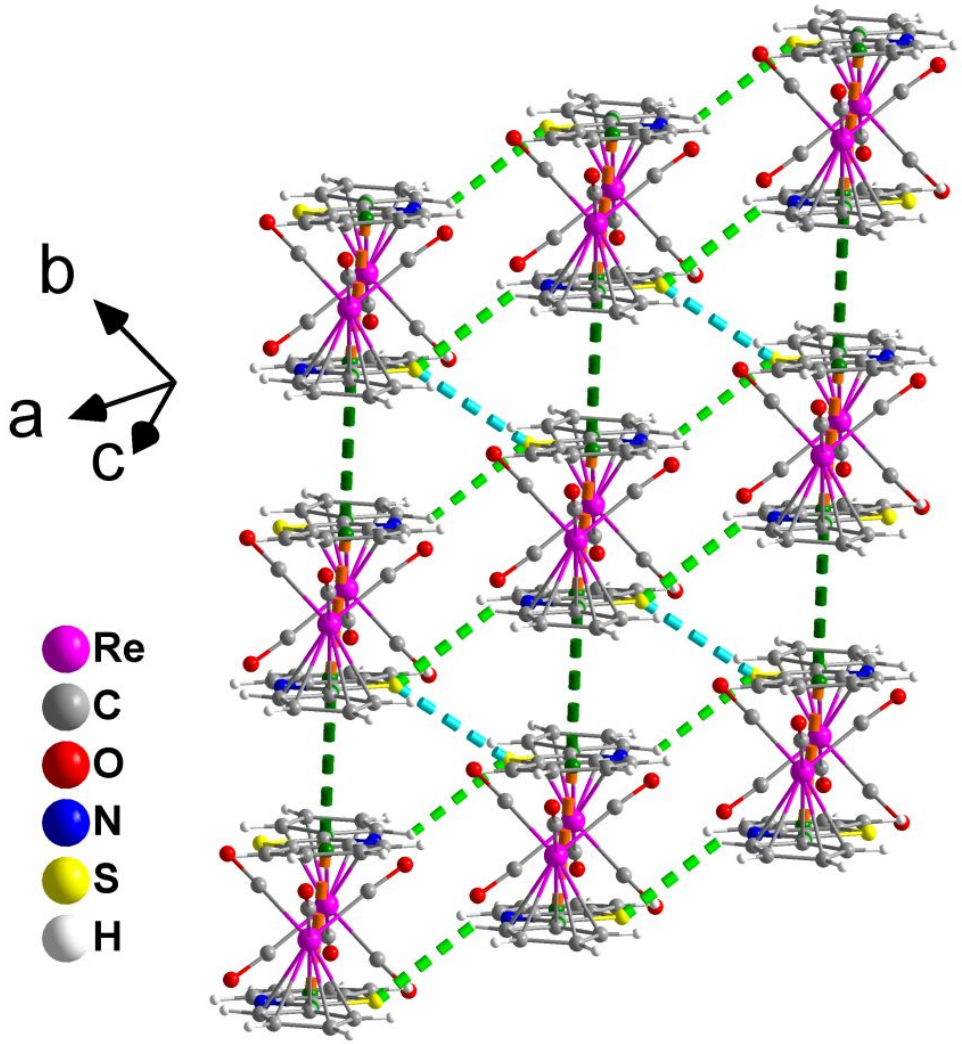

Figure S7. Layer of clusters in the structure of **Re-1**. Dashed orange lines represent π ···π intradimer interactions of the phenyl ringsand and dark green interdimer one. Dashed cyan and dashed light green lines represent S1···S1 and C4-H4···S1 type of interactions respectively.

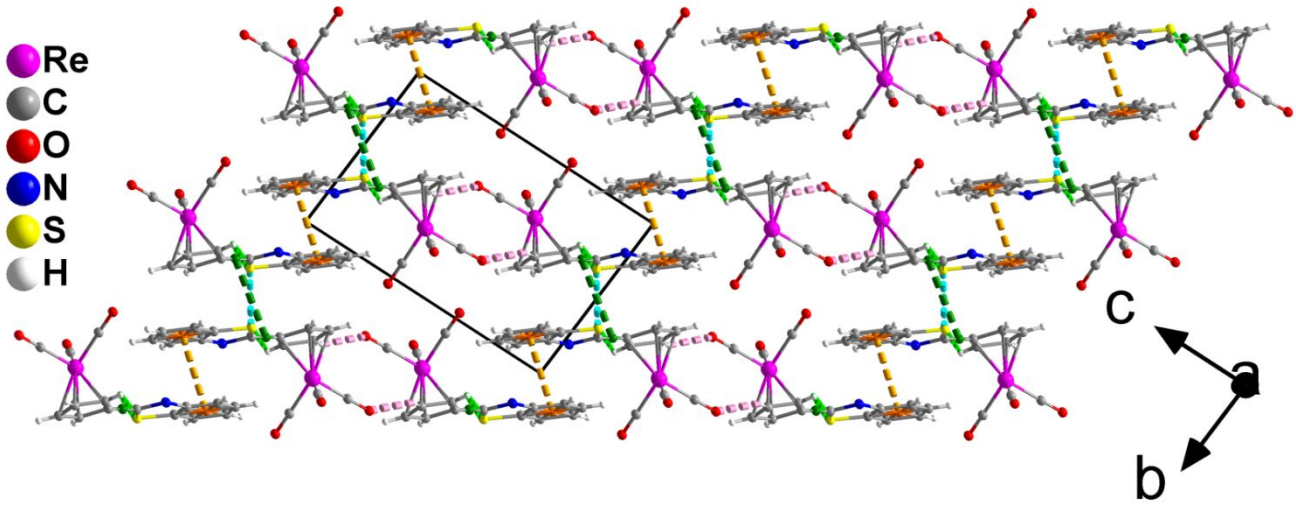

Figure S8. 3D Arrangement of clusters in the structure of **Re-1**. Dashed orange lines represent π ···π intradimer interactions of the phenyl rings and dark green interdimer one. Dashed cyan, light green and pink lines represent S1···S1, C4-H4···S1 and C5-H5···O2 type of interactions respectively.

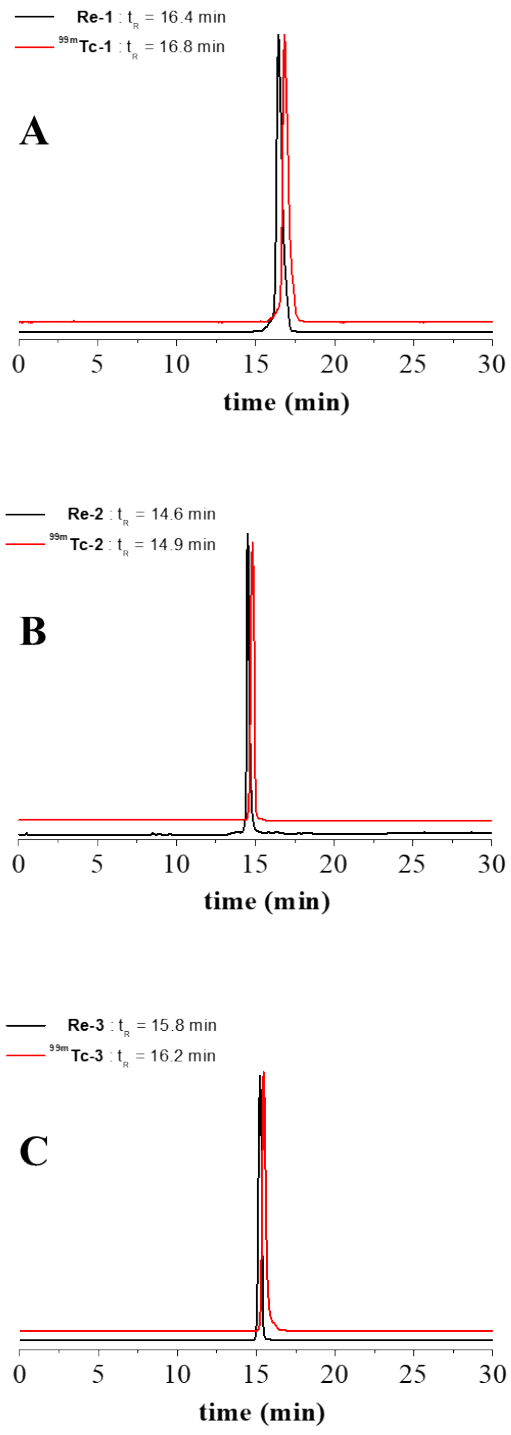

Figure S9. Reverse-phase HPLC chromatograms of Re (photometric detection) and ^{99m}Tc complexes (radiometric detection) for A) **Re-1** and **^{99m}Tc-1**, B) **Re-2** and **^{99m}Tc-2**, and C) **Re-3** and **^{99m}Tc-3**.

Table S5. Stability of ^{99m}Tc complexes at 37 °C against histidine and cysteine and stability of the Re complexes in cell culture medium

Stability								
	in the presence of histidine			**in the presence of cysteine**				**in cell medium**
	1 h	**3 h**	**6 h**	**1 h**	**3 h**	**6 h**		**24 h**
^{99m}Tc-1	98 ± 1	97 ± 1	97 ± 1	98 ± 1	97 ± 2	97 ± 1	**Re-1**	99 ± 1
^{99m}Tc-2	98 ± 1	98 ± 1	97 ± 1	98 ± 1	98 ± 1	97 ± 2	**Re-2**	99 ± 1
^{99m}Tc-3	98 ± 1	96± 1	95± 1	98± 1	95± 2	85± 1	**Re-3**	99 ± 1

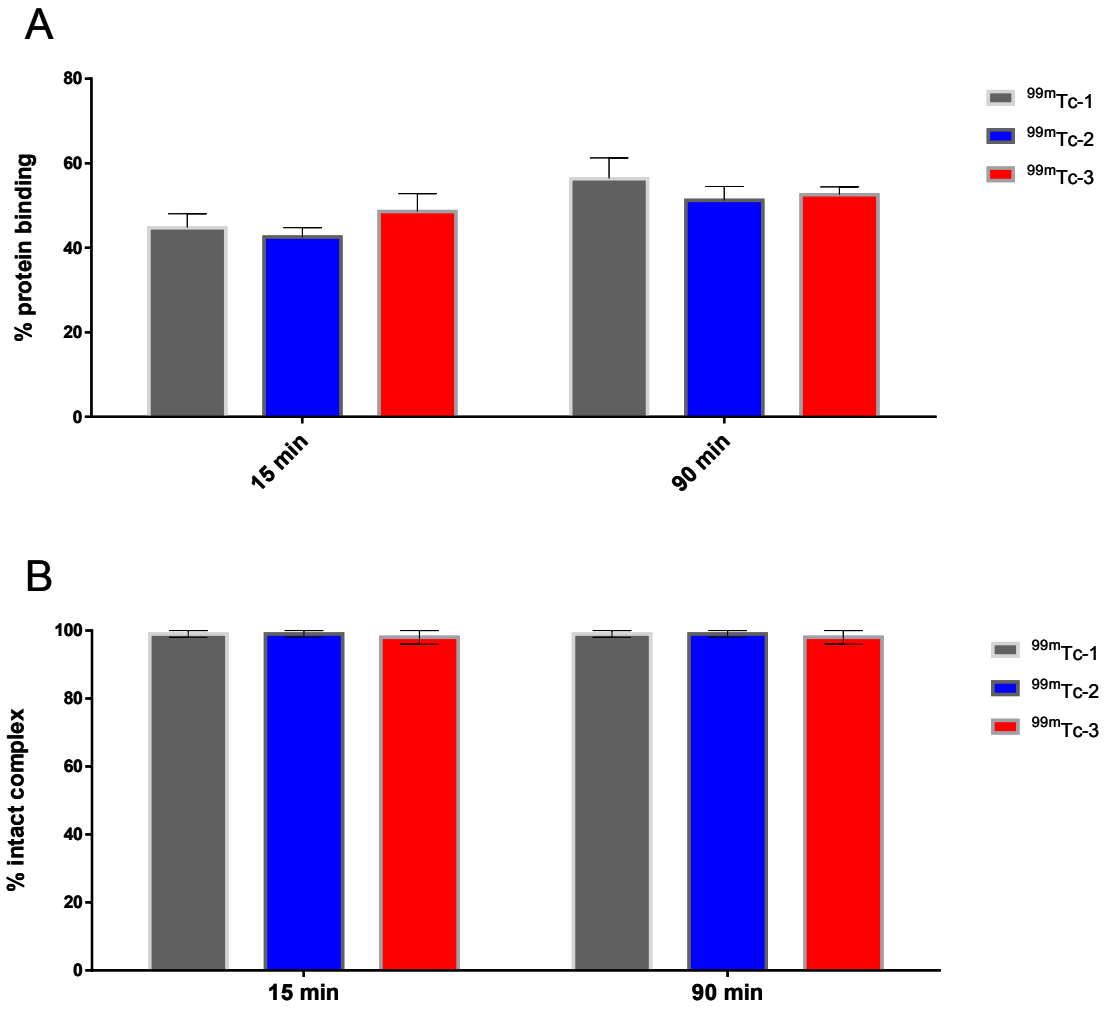

Figure S10. (A) Percentage of binding (% binding) of the ^{99m}Tc complexes to plasma proteins, after incubation with rat plasma for 15 min and 90 min, at 37 °C. Shown are mean values ± SDs from three experiments. (B) Stability of the ^{99m}Tc complexes after 15 and 90 min incubation with rat plasma at 37 °C.

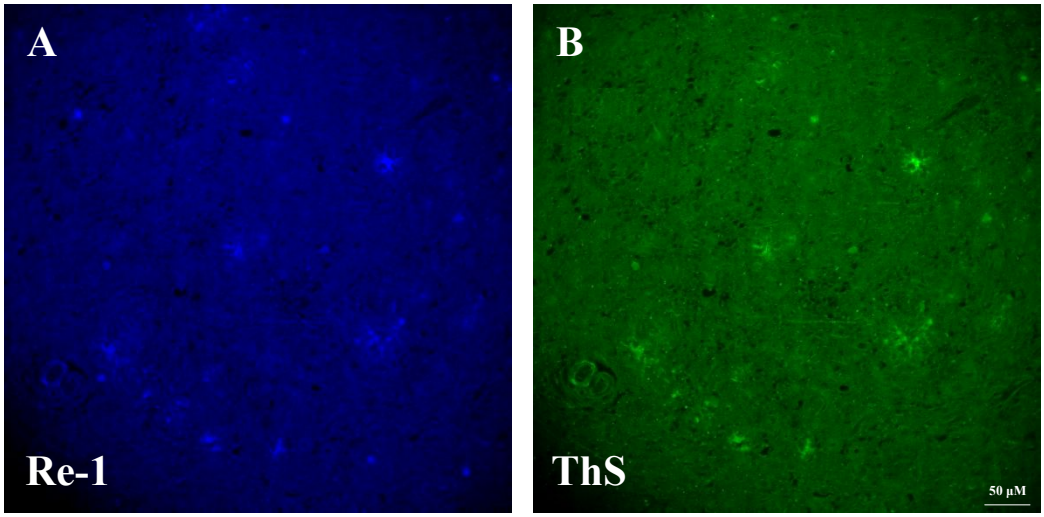

Figure S11. Confocal fluorescence images (λ_{exc} 370 nm, λ_{em} 580 nm) of consecutive brain slices from an autopsy confirmed AD patient stained with complex (A) **Re-1** and (B) ThS as a positive control. The scale bar corresponds to 50 µm.

Table S6. Biodistribution of radioactivity (% ID/g) a 15 min after injection of complex **^{99m}Tc-1** in transgenic 5xFAD (Tg) mice (n = 4) and in their wild type (wt) littermates (n = 4)[a].

^{99m}Tc-1		
	Tg	**wt**
organ	15 min	15 min
blood	1.51 ± 0.24	1.54 ± 0.23
liver	19.08 ± 3.03	19.18 ± 3.84
heart	5.84 ± 1.96	3.20 ± 0.56
kidneys	11.34 ± 0.96	12.21 ± 2.14
stomach	4.13 ± 3.55	11.05 ± 6.84
intestines	10.16 ± 2.07	8.11 ± 1.14
spleen	3.63 ± 1.26	2.21 ± 0.32
muscle	2.99 ± 0.32	2.11 ± 0.55
lungs	14.96 ± 1.85	10.87 ± 0.63
pancreas	4.93 ± 0.96	3.90 ± 1.16
brain	3.90 ± 0.19	2.68 ± 0.06

[a]All data are expressed as the % of the injected dose per gram of wet tissue ± the standard deviation of the mean.

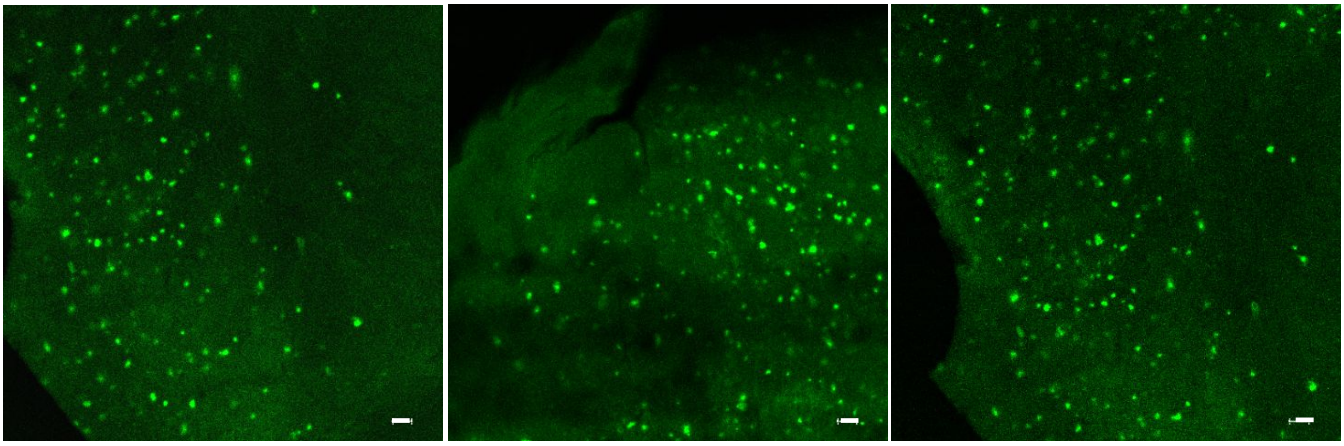

Figure S12. *In vitro* fluorescent staining with Thioflavin S of brain slices from three Tg 5xFAD mice for confirmation of the presence of amyloid plaques by confocal microscopy (λ_{exc} 370 nm, λ_{em} 580 nm). The scale bar corresponds to 50 μm.

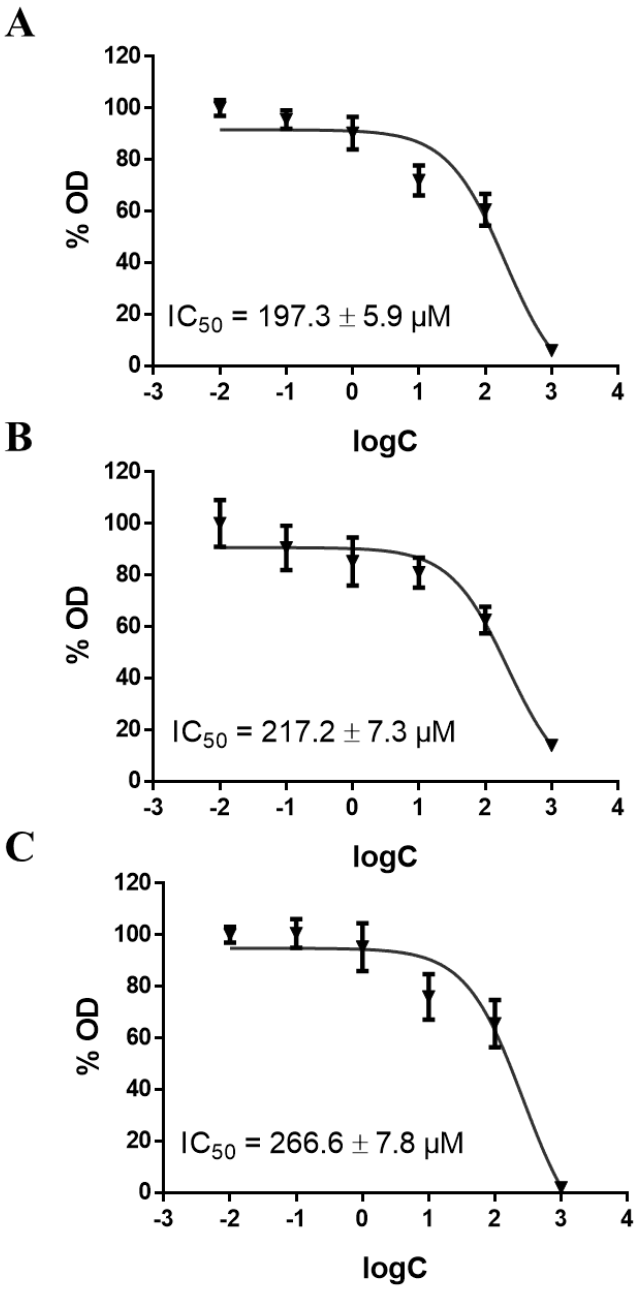

Figure S13. MTT assay curves for complexes (A) **Re-1**, (B) **Re-2** and (C) **Re-3b** against U87MG cells (72 h exposure). The calculated IC_{50} (μM) values indicate relatively low toxicity of Re complexes. Each experiment was repeated three times and in every run each concentration was used in quadruplicate (n = 4).

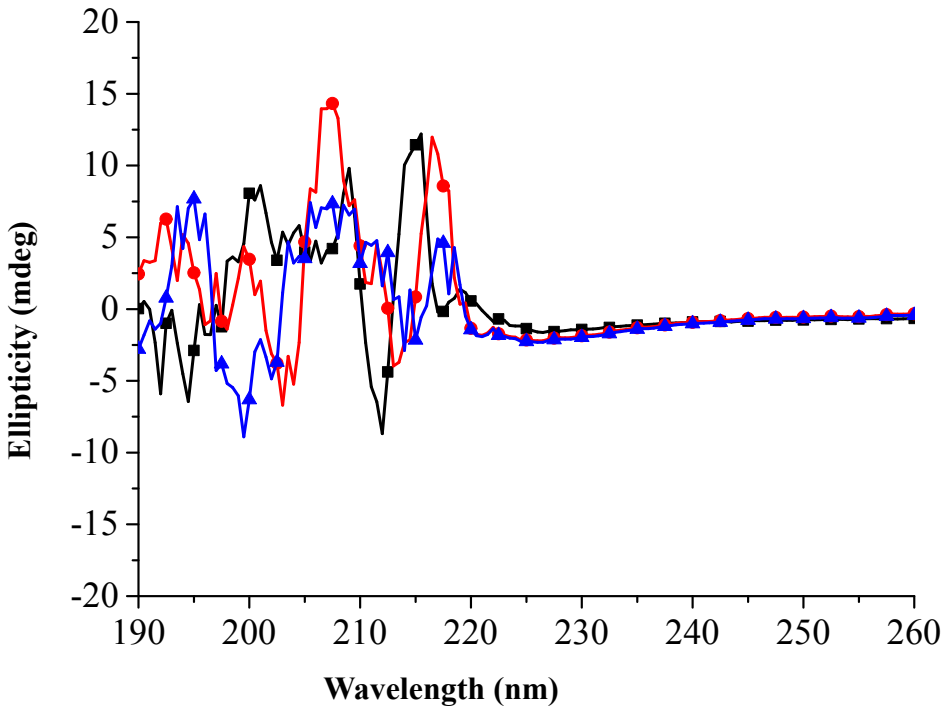

Figure S14. CD spectra of plain **Re-1** (black line), **Re-2** (red line) and **Re-3** (blue line) complexes at a concentration of 50 μM in PBS. The spectra remained noisy even down to the concentration of 6 μM which is the lowest limit for monitoring Aβ interactions under our experimental conditions.

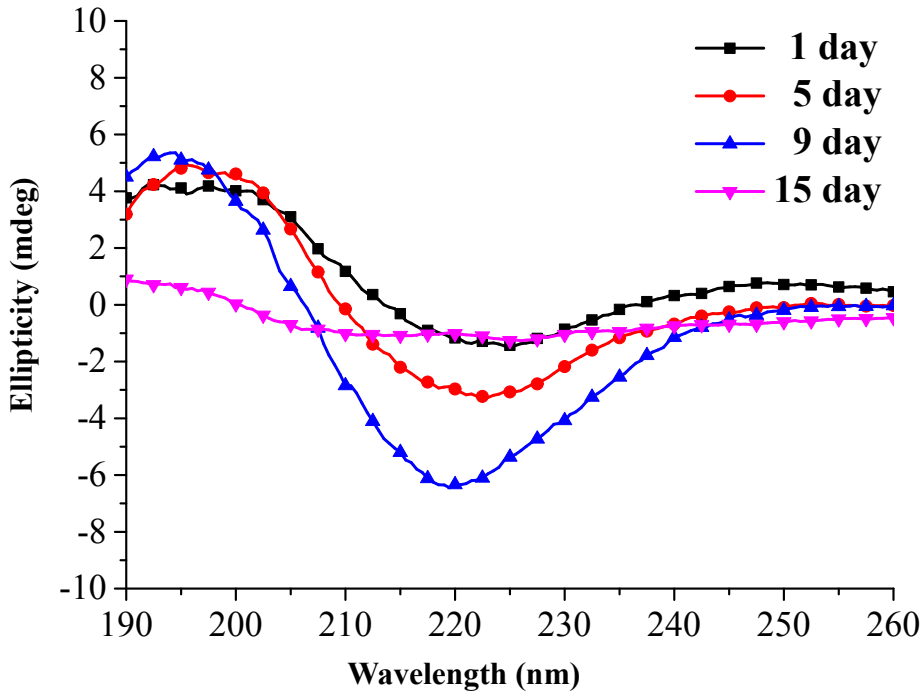

Figure S15. CD spectra of Aβ42 in PBS (50 μM) over a period of 15 days. The spectra reflect the conformational changes that Aβ42 undergoes from *β*-sheet oligomeric forms to higher *β*-sheet pre-fibrillar forms, and eventually to *β*-amyloid fibrils that precipitate from solution, resulting in loss of signal (pink line, day 15).